

Scheme 1. The *N*-alkyl-protonated Schiff base of retinal (PSBR).

Computer Chemistry

DOI: 10.1002/ange.200501236

A Tiny Excited-State Barrier Can Induce a Multiexponential Decay of the Retinal Chromophore: A Quantum Dynamics Investigation**

Massimo Olivucci,* Alessandro Lami, and Fabrizio Santoro**

The *N*-alkyl protonated Schiff base of retinal (PSBR) is the chromophore of rhodopsin proteins,^[1–3] a large class of transmembrane photoreceptors comprising the human retina visual pigment rhodopsin (Rh) and the bacterial proton pump bacteriorhodopsin (bR). In these receptors, PSBR undergoes an efficient *cis*–*trans* photoisomerization (e.g., the 11-*cis* to all-*trans* isomerization marked with a curved arrow in Scheme 1) which, ultimately, triggers a conformational change of the protein. It has been established that in solution the excited-state decay of PSBR is multiexponential and shows a fast (subpicosecond to picosecond) and a slow (picosecond) component, whose values depend on the type of signal recorded, the probing wavelength, and the

nature of the solvent.^[4–7] More recently, evidence for multiexponential excited-state decay has also been reported for Rh^[8,9] and bR.^[10]

The precise origin of the observed PSBR multiexponential decay is unknown. Several models have been proposed such as the existence of competing excited-state isomerization paths^[7] (for example, one reactive and one nonreactive path as demonstrated in ref. [9]) or the occurrence of an isomerization path splitting,^[8] or the generation of a vibrationally hot photoproduct followed by cooling.^[11] The possibility that a multiexponential decay arises from dynamics along a single coordinate has also been discussed.^[12] Herein, we present an investigation on a different origin of multiexponential decay: the dynamics prompted by the specific shape of the excited-state potential-energy surface.

Ab initio CASPT2//CASSCF calculations on the reaction path of different isolated PSBR models,^[13–16] and more recently on Rh,^[17] have invariably shown that the isomerization path on the excited state (*S*₁) involves mainly two nuclear modes. The process begins with the relaxation of the Franck–Condon (FC) structure along a collective C–C stretching (double-bond expansion and single-bond contraction) mode of the chromophore backbone. It then proceeds along the torsion corresponding to the change from *cis* to *trans*; this torsion leads to a conical intersection (CI) between the *S*₁ and the ground-state (*S*₀) potential-energy surfaces. The essential features of the calculated surface, which are in line with the indication of time-resolved experiments,^[18–24] are reproduced by the simple analytical potential *V*^C [Eq. (1)]

$$V^C(x_s, y_t) = a_s x_s^2 - b_t (x_s/x_{\text{seq}}) y_t^2 \quad (1)$$

with $b_t > 0$.^[25] As illustrated in Figure 1 a, a vibrational wave packet released at FC initially evolves along the stretching coordinate x_s . *V*^C is bound along y_t when $x_s < 0$, but it is unbound (i.e., gives the wave packet an acceleration towards large y_t values) when $x_s > 0$ (Figure 1 b). This anharmonic feature creates a shallow valley around the origin (SP) and, for $x_s > 0$, a decay channel along y_t , whose existence has been documented by mapping the minimum-energy path for realistic PSBR models.^[16] *V*^C does not describe the region of the conical intersection, which must be thought somewhere along the channels. Below, we assume that once the wave packet is entered into the decay channels, it will irreversibly proceed towards the CI and decay to *S*₀.

Because of its low dimensionality *V*^C provides an attractive model for the study of the quantum dynamics of the photoinduced wave packet. While we do not try to reproduce experimental data, we show that the peculiar topology of the *S*₁ energy surface of PSBR may be responsible for biexponential decay. In particular, we show that such a decay regime

[*] Prof. Dr. M. Olivucci
Dipartimento di Chimica
Università degli Studi di Siena
via Aldo Moro, 53100 Siena (Italy)
Fax: (+39) 577-234-278
and Centro Studio Sistemi Complessi
via Tommaso Pendola 37, 53100 Siena (Italy)
E-mail: olivucci@unisi.it

Prof. Dr. M. Olivucci, Dr. A. Lami, Dr. F. Santoro
Istituto per i Processi Chimico-Fisici
Area della Ricerca del CNR di Pisa
via Moruzzi 1, 56124 Pisa (Italy)
Fax: (+39) 50-315-2442
E-mail: f.santoro@ipcf.cnr.it

[**] We thank Dr. G. Granucci of Università di Pisa for valuable discussion on classical simulation of wave-packet dynamics. M.O. acknowledges the Università di Siena (Progetto di Ateneo 02/04), HFSP (RG 0229/2000M), and FIRB (project No. RBAU01EPMR) for providing the funds.

Supporting information for this article is available on the WWW under <http://www.angewandte.org> or from the author.

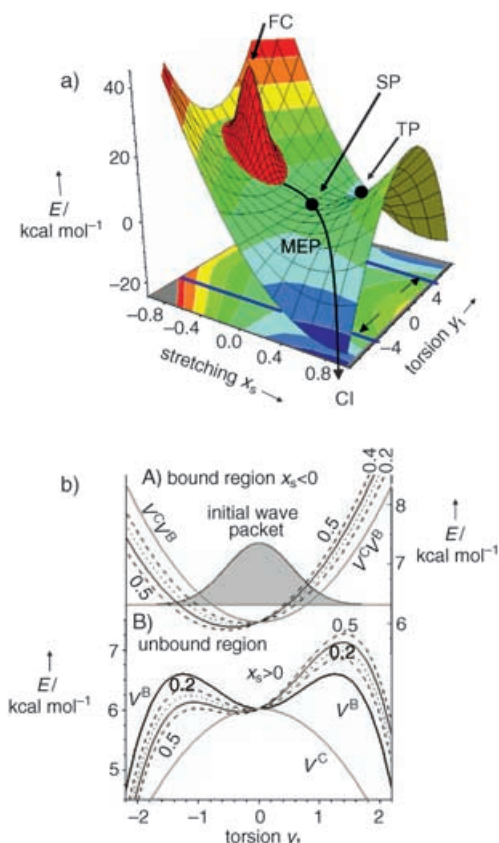


Figure 1. a) 3D plot of the potential V^c ; the initial wave packet at $t=0$ is superimposed. x_s and y_t are given in atomic units. Two lines on the $x_s y_t$ plane mark the borders of the NR region ($-4 \text{ au} \leq y_t \leq 4 \text{ au}$). The curved arrow indicates the minimum-energy path (labeled MEP) towards negative values of y_t (an equivalent MEP develops towards positive values of y_t). b) Profiles of the potential with no barrier (V^c), with a symmetric barrier (V^b), and with an asymmetric barrier (asymmetry parameter c_t : 0.2, 0.3, 0.4, 0.5 kcal mol⁻¹ bohr⁻¹). A) $x_s = -0.475 \text{ au}$ (FC); the larger c_t the more shifted the minimum is towards negative y_t values. The cross section of the initial wave packet is given as a gray Gaussian. B) $x_s = 0.475 \text{ au}$ (TP); the larger c_t the higher the barrier for positive y_t and the lower the barrier for negative y_t .

is induced by the presence of a flat energy ridge located between the SP and CI regions.

We begin by looking at a barrierless potential. The parameters of Equation (1) are fixed by assuming typical values for pure stretching ($\omega_s = 1500 \text{ cm}^{-1}$, $a_s = 1/2 m_s \omega_s^2$, $m_s = 1 \text{ u}$; $\text{u} = \text{atomic mass unit}$, $\omega = \bar{\nu}$) and torsional frequencies ($\omega_t = 200 \text{ cm}^{-1}$, $b_t = 1/2 m_t \omega_t^2$, $m_t = 1 \text{ u}$). The FC point is located at $x_s(0) = x_{\text{seq}} = -0.475 \text{ au}$ by imposing an energy gap of 6 kcal mol⁻¹ between the points FC and SP, which is consistent with the results of ab initio calculations.^[15] To study how the wave packet moves along the SP→CI channel, we monitor $P_{\text{NR}}(t)$, which describes the population in the nonreactive (NR) region comprising FC and SP (see Figure 1 a) or, in other words, the transient S₁ population of PSBR. The results (see the thick gray line in Figure 2 a, b) demonstrate that after

an induction time of about 50 fs there is a substantial monoexponential decay of $P_{\text{NR}}(t)$ with a time constant of about 150 fs (see the Supporting Information for a table with the exponential fits of $P_{\text{NR}}(t)$ for the S₁ potential).

The presence of a barrier < 1 kcal mol⁻¹ on the S₁ surface has been detected experimentally^[6] and is consistent with CASPT2//CASSCF calculations on a realistic PSBR model.^[16] We now show that energy ridges (Figure 2 c, dotted lines)—which start at $x_s = 0$ and $y_t = \pm 1.26 \text{ au}$, increase linearly for $x_s > 0$ (along the stretching), and impose a tiny torsional barrier (B^{max} of 0.6 kcal mol⁻¹ at the turning-point (TP) level (see V^b Figure 1 b, plot B)—have a drastic effect on the decay dynamics. Naming V^b the potential with a barrier (see the Supporting Information for mathematical details), we report in Figures 2 a and b the $P_{\text{NR}}(t)$ function. As apparent from an inspection of the graphs, the barrier switches the S₁ population decay from monoexponential to biexponential with time constants of 257 fs (19% of the population) and 2110 fs (81% of the population). The appearance of the biexponential decay does not depend on a specific choice of the V^b parameters; for example, the biexponential decay persists if the barrier is moved along y_t between 0.8 and 1.5 au and its height is fixed to the value of 0.6 kcal mol⁻¹ (the time constants and the populations of the fast and slow components vary significantly). Furthermore, the extension of the ridge to negative x_s values, which creates a barrier along the MEP, should prompt the biexponential regime more readily.

Figure 2 c provides a mechanistic interpretation of the biexponential regime. The tiny barrier in the region of the

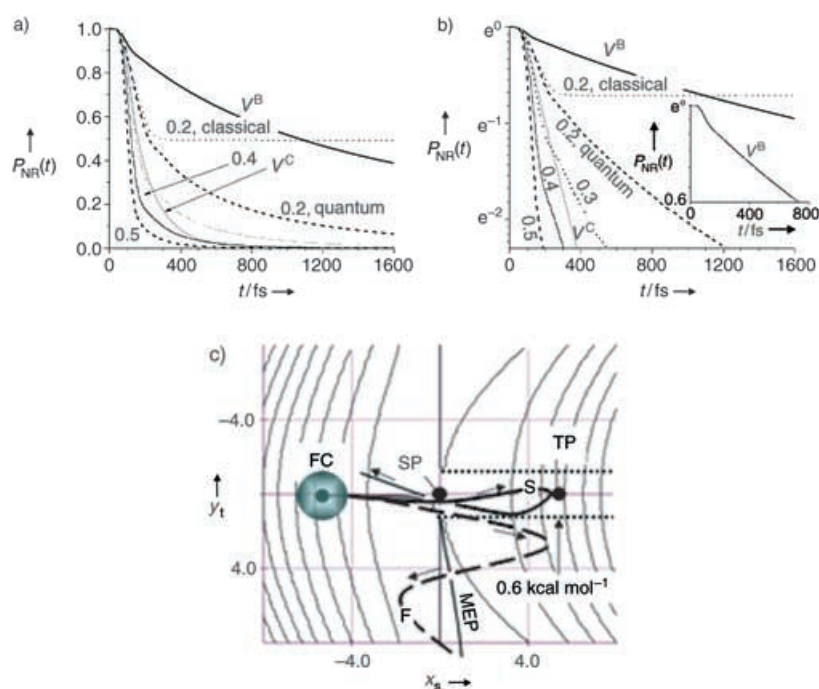


Figure 2. Decay of the quantum NR population, $P_{\text{NR}}(t)$: a) linear scale; b) semilogarithmic scale. Potentials V^c (thick gray line), V^b (solid line), and $V^b + c_t y_t$ (curves marked by the c_t values 0.2, 0.3, 0.4, 0.5 kcal mol⁻¹ bohr⁻¹; for $c_t = 0.2$ the classical result is also given). Notice that the larger c_t the faster the decay. Inset: detail of the decay for V^b . c) Schematic representation of a fast (F) and slow (S) trajectory on a contour plot of V^c . The positions of the V^b energy ridges are marked by two dotted lines.

turning point restrains the decay of a large subset of trajectories that temporarily remain in the NR region (S trajectory) rather than evolve immediately along the SP→CI channel (F trajectory). However, the introduction of a barrier does not cause an “isomerization path splitting”. In fact, the wave packet oscillates along the stretching mode in the SP region without splitting. What actually happens is a progressive loss of population of the NR region that enters the SP→CI channel of no return (for an analysis of the flow of the population in the SP→CI channel as a function of the stretching x_s see the Supporting Information).

The investigation of the origin of the biexponential decay in the protein environment (e.g., in Rh^[8,9] or bR^[10]) requires the detailed understanding of the PSBR V^B topology in these systems. While this is outside the scope of the present work, we can easily introduce in V^B the zero-order effect of the chiral protein cavity, that is, the breaking of the mirror symmetry of the torsional potential. This is done through an additional term, $c_t y_t$, which shifts the equilibrium position along y_t , removes the symmetry of the barriers for positive torsion values (B_+^{\max}) and for negative torsion values (B_-^{\max}), and decreases the size of the SP valley (see Figure 1 b and the Supporting Information).

In Figure 2 a,b, we report the changes of $P_{NR}(t)$ as a function of the increase of the asymmetry parameter c_t . It is apparent that even when c_t induces a limited symmetry breaking (see Figure 1 b and the Supporting Information), both time constants of the biexponential fit decrease (i.e., the overall decay is faster) and more remarkably the population decay with the faster kinetic increases while the population decay with the slower kinetic decreases (for $c_t = 0.2$ kcal·mol⁻¹·bohr⁻¹ these are 62% for the fast decay and 38% for the slow decay). When $c_t = 0.5$ kcal·mol⁻¹·bohr⁻¹ the slow component disappears and the biexponential fit collapses into the monoexponential one with a time constant of 72 fs. These results show that, according to our basic model, the symmetry breaking induced by the protein cavity would decrease the multiexponential character of the decay, which would ultimately lead to a monoexponential behavior due to the removal of the plateau around SP and the decrease of the barrier along one sense of rotation ($B_-^{\max} < B_+^{\max}$ in Figure 1 b).

The comparison between quantum and classical $P_{NR}(t)$ for the case $c_t = 0.2$ kcal·mol⁻¹·bohr⁻¹ (see Figures 2 a,b) demonstrates that quantum effects, like tunneling, are essential for the correct description of the slower decay of the NR population. In fact, classical trajectories (see the Supporting Information) do not reproduce the behavior described above but predict that after the fast decay, a part of the wave packet remains unreactive and is permanently trapped on the SP valley.

In conclusion, exploratory quantum dynamics on a two-dimensional analytical potential that mimics the PSBR S_1 potential derived through ab initio quantum chemical calculations provides a novel explanation for the observed biexponential decay of the excited-state population. Such an explanation may be proposed for other systems featuring a biexponential decay with a fast component in the sub-picosecond regime. The motion of the wave packet is strongly affected by the existence of a tiny barrier along the channel

leading to the conical intersection. This phenomenon is general (as an example it still survives for $\omega_s \approx 700$ cm⁻¹ and $\omega_s \approx 500$ cm⁻¹) and depends on the topology of the S_1 surface. The sensitivity of the quantum dynamics of the wave packet to the precise features of the potential is also reflected by the chaotic behavior found for classical trajectories released on V^C . This fact and other details of the investigation reported above will be documented in a forthcoming publication.

Experimental Procedure

Quantum dynamical calculations were performed assuming the simple kinetic operator $T = (2m_s)^{-1} \partial^2 / \partial x_s^2 + (2m_t)^{-1} \partial^2 / \partial y_t^2$ ($m_s = m_t = 1$ u) by adopting the Fourier method,^[26] and propagating the wave packet through an orthogonalized Lanczos algorithm.^[27,28] We assume an FC excitation from the ground (harmonic) vibrational state of the S_0 surface to S_1 and equal frequencies on the S_0 (ω'_s, ω'_t) and S_1 (ω_s, ω_t) surfaces ($\omega'_s = \omega_s, \omega'_t = \omega_t$). An initial thermal distribution of the torsional states increases, moderately, the population of the fast component of the biexponential decay.

Supporting Information includes: Computational details; a mathematical expression for the V^B potential; a table of the exponential fits of quantum $P_{NR}(t)$ for different values of the S_1 potential; a table reporting the positions and heights of the barriers for the different potentials considered and the comparison between mono- and biexponential fits; further discussion of the reaction mechanism through the analysis of snapshots of the wave packet and through the study of the $P_{NR}(t)$ decay as a function of x_s .

Received: April 8, 2005

Published online: July 20, 2005

Keywords: ab initio calculations · isomerization · photochemistry · Schiff bases

- [1] R. A. Mathies, J. Lutheburg in *Handbook of Biological Physics*, Vol. 3 (Eds.: D. G. Stavenga, W. J. De Grip, E. N. Pugh), Elsevier Science, New York, **2000**.
- [2] R. Needlman in *CRC Handbook of Organic Photochemistry and Photobiology* (Eds.: W. M. Horspool, P.-S. Song), CRC, Boca Raton, FL, **1995**.
- [3] M. Ottolenghi, M. Sheves, *Isr. J. Chem.* **1995**, 35, 193.
- [4] H. Kandori, H. Sasabe, *Chem. Phys. Lett.* **1993**, 216, 126.
- [5] P. Hamm, M. Zurek, T. Röslinger, H. Patzelt, D. Oesterhelt, W. Zinth, *Chem. Phys. Lett.* **1996**, 263, 613.
- [6] S. L. Logunov, L. Song, M. A. El-Sayed, *J. Phys. Chem.* **1996**, 100, 18586.
- [7] G. Zgrablic, K. Voitchovsky, M. Kindermann, M. Chergui, S. Haacke in *Femtochemistry and Femtobiology: Ultrafast Events in Molecular Science* (Eds.: M. Martin, J. T. Hynes), Elsevier Science, New York, **2004**, pp. 457–460.
- [8] M. Yan, L. Rothberg, R. Callender, *J. Phys. Chem. B* **2001**, 105, 856–859.
- [9] H. Kandori, Y. Furutani, S. Nishimura, Y. Shichida, H. Chosrowjan, Y. Shibata, N. Mataga, *Chem. Phys. Lett.* **2001**, 334, 271–276.
- [10] S. Schenkl, E. Portuondo, G. Zgrablic, M. Chergui, S. Haacke, N. Friedman, M. Sheves, *Phys. Chem. Chem. Phys.* **2002**, 4, 5020–5024.
- [11] J. E. Kim, D. W. McCamant, L. Zhu, R. A. Mathies, *J. Phys. Chem. B* **2001**, 105, 1240–1249.
- [12] M. Du, G. R. Fleming, *Biophys. Chem.* **1993**, 48, 101.
- [13] L. De Vico, C. S. Page, M. Garavelli, F. Bernardi, R. Basosi, M. Olivucci, *J. Am. Chem. Soc.* **2002**, 124, 4124–4134.

- [14] M. Garavelli, P. Celani, F. Bernardi, M. A. Robb, M. Olivucci, *J. Am. Chem. Soc.* **1997**, *119*, 6891–6901.
- [15] M. Garavelli, T. Vreven, P. Celani, F. Bernardi, M. A. Robb, M. Olivucci, *J. Am. Chem. Soc.* **1998**, *120*, 1285–1288.
- [16] R. Gonzalez-Luque, M. Garavelli, F. Bernardi, M. Merchán, M. A. Robb, M. Olivucci, *Proc. Natl. Acad. Sci. USA* **2000**, *97*, 9379–9384.
- [17] T. Andruniów, N. Ferré, M. Olivucci, *Proc. Natl. Acad. Sci. USA* **2004**, *101*, 17908–17913.
- [18] a) Q. Zhong, S. Ruhman, M. Ottolenghi, *J. Am. Chem. Soc.* **1996**, *118*, 12828–12829; b) B. Hou, N. Friedman, S. Ruhman, M. Sheves, M. Ottolenghi, *J. Phys. Chem. B* **2001**, *105*, 7042–7048.
- [19] G. Haran, K. Wynne, A. Xie, Q. He, M. Chance, R. M. Hochstrasser, *Chem. Phys. Lett.* **1996**, *261*, 389–395.
- [20] L. Song, M. A. El-Sayed, *J. Am. Chem. Soc.* **1998**, *120*, 8889–8890.
- [21] T. Kakitani, R. Akiyama, Y. Hatano, Y. Imamoto, Y. Shichida, P. Verdegem, J. Lugtenburg, *J. Phys. Chem. B* **1998**, *102*, 1334–1339.
- [22] G. Haran, E. A. Morlino, J. Matthes, R. H. Callander, R. M. Hochstrasser, *J. Phys. Chem. A* **1999**, *103*, 2202–2207.
- [23] S. Haacke, S. Vinzani, S. Schenkl, M. Chergui, *ChemPhysChem* **2001**, *2*, 310–315.
- [24] T. Kobayashi, T. Saito, H. Ohtani, *Nature* **2001**, *414*, 531–534.
- [25] A. Cembran, F. Bernardi, M. Olivucci, M. Garavelli, *J. Am. Chem. Soc.* **2003**, *125*, 12509.
- [26] R. Kosloff in *Dynamics of Molecules and Chemical Reactions* (Eds.: R. E. Wyatt, J. Z. H. Zhang), Marcel Dekker, New York, **1996**.
- [27] C. Lanczos, *Natl. Bur. Stand. Circ.* **1950**, *45*, 225.
- [28] A. Ferretti, G. Granucci, A. Lami, M. Persico, G. Villani, *J. Chem. Phys.* **1996**, *104*, 5517.